arXiv:1407.0533v2 [math.NA] 17 Jul 2014

Sampling by incomplete cosine expansion of the sinc function: application to the Voigt/complex error function

S. M. Abrarov* **and B. M. Quine***†

July 17, 2014

Abstract

A new sampling methodology based on incomplete cosine expansion series is presented as an alternative to the traditional sinc function approach. Numerical integration shows that this methodology is efficient and practical. Applying the incomplete cosine expansion we obtain a rational approximation of the complex error function that with the same number of the summation terms provides an accuracy exceeding the Weideman's approximation accuracy by several orders of the magnitude. Application of the expansion results in an integration consisting of elementary function terms only. Consequently, this approach can be advantageous for accurate and rapid computation.

Keywords: sinc function, sampling, numerical integration, complex error function, Voigt function, plasma dispersion function, rational approximation

1 Introduction

Sinc function is defined as [10]

$$\operatorname{sinc}(t) \equiv \begin{cases} \dfrac{\sin(t)}{t}, & t \neq 0 \\ 1, & t = 0. \end{cases}$$

*Dept. Earth and Space Science and Engineering, York University, Toronto, Canada, M3J 1P3.
†Dept. Physics and Astronomy, York University, Toronto, Canada, M3J 1P3.

Sinc function is widely used in practical applications due to its remarkable sampling property [29]. In particular, using the sinc function we can approximate a function $f(t)$ by taking appropriate set of the sampling points $\{t_n, f(t_n)\}$ along some interval $[a, b]$ as [26, 17]:

$$f(t) = \sum_{n=-N}^{N} f(t_n) \operatorname{sinc}\left(\frac{\pi}{h}(t - t_n)\right) + \varepsilon(t), \tag{1}$$

where $2N+1$ is the total number of the sapling points, h is the small parameter and $\varepsilon(t)$ is the error term. This remarkable sampling property of the sinc function can be used, for example, in numerical integration or differentiation [29].

Although according to equation (1) the sinc function can approximate quite accurately a function by sampling, its application is not always practically convenient. For example, suppose that $f(t, x, y, z...)$ is a multivariable function and suppose that it can be represented as a multiplication of two functions $f(t, x, y, z...) = g(t) h(t, x, y, z...)$. Then the expansion of the function $g(t)$ in terms of sinc function series (1) leads to sum of integrals of kind

$$\int_a^b f(t, x, y, z...)\, dt \approx \sum_{n=-N}^{N} \int_a^b g(t_n) \operatorname{sinc}\left(\frac{\pi}{h}(t - t_n)\right) h(t, x, y, z...)\, dt \tag{2}$$

that may not be necessarily integrable or expressed in terms of the rational functions for efficient computation since the sinc function is not an elementary function.

It this work we propose a methodology of sampling based on the incomplete cosine expansion series of the sinc function that effectively resolves this problem and, as an example, we demonstrate its effectiveness in derivation of a new approximation of the Voigt/complex error function where only 16 summation terms are sufficient to obtain accuracy better than 10^{-12} over almost all the complex domain of practical importance. This example illustrates how the incomplete cosine expansion of the sinc function can be applied as a useful and versatile technique in numerical integration.

2 Sampling methodology

2.1 Incomplete cosine expansion

Viéta discovered that the sinc function can be represented as infinite product of the cosine functions [10, 15]:

$$\operatorname{sinc}(t) = \prod_{m=1}^{\infty} \cos\left(\frac{t}{2^m}\right). \tag{3}$$

There is a product-to-sum identity [23]

$$\prod_{m=1}^{M} \cos\left(\frac{t}{2^m}\right) \equiv \frac{1}{2^{M-1}} \sum_{m=1}^{2^{M-1}} \cos\left(\frac{2m-1}{2^M} t\right), \tag{4}$$

where M is an integer. Comparing identities (3) and (4) we can conclude, therefore, that

$$\operatorname{sinc}(t) = \lim_{M\to\infty} \frac{1}{2^{M-1}} \sum_{m=1}^{2^{M-1}} \cos\left(\frac{2m-1}{2^M} t\right).$$

Consequently, at any finite integer M we can refer to the right side of equation (4) as incomplete cosine expansion of the sinc function.

In sampling techniques involving the sinc function, it is quite common to replace its argument as $t \to \pi t/h$ (see for example [26, 17]). Following this convention, we rewrite the incomplete cosine expansion of the sinc function as the series

$$\frac{1}{2^{M-1}} \sum_{m=1}^{2^{M-1}} \cos\left(\frac{\pi\,(2m-1)}{2^M h} t\right). \tag{5}$$

One useful property of this expansion occurs at infinitesimal h:

$$\lim_{h\to 0} \lim_{M\to\infty} \frac{1}{2^{M-1}} \sum_{m=1}^{2^{M-1}} \cos\left(\frac{\pi\,(2m-1)}{2^M h} t\right) \equiv \delta(t)$$

where $\delta(t)$ is the Kronecker delta, equal to 1 at $t = 0$ and equal to 0 at $t \neq 0$. This interesting behaviour can be proved from the observation that:

$$\lim_{h\to 0} \operatorname{sinc}\left(\frac{\pi}{h} t\right) \equiv \delta(t).$$

Since the integer M in this application is implied to be finite, the incomplete cosine expansion (5) is a periodic function with period T that is dependent upon the values M and h. A larger value of the integer M increases the number of the summation terms in the incomplete cosine expansion (5) that leads to an increase of the period T.

As the incomplete cosine expansion approximates the original sinc function $\operatorname{sinc}(\pi t/h)$ within the range $t \in [-T/4, T/4]$ near the origin, we can write the approximation as

$$\frac{1}{2^{M-1}} \sum_{m=1}^{2^{M-1}} \cos\left(\frac{\pi\,(2m-1)}{2^M h} t\right) \approx \operatorname{sinc}\left(\frac{\pi}{h} t\right), \qquad -T/4 \le t \le T/4. \tag{6}$$

Figure 1 shows the results calculated at $M = 5$ and $h = 0.25$. The period of the incomplete cosine expansion is $T = 16$. For comparison the original sinc function is also shown by blue line.

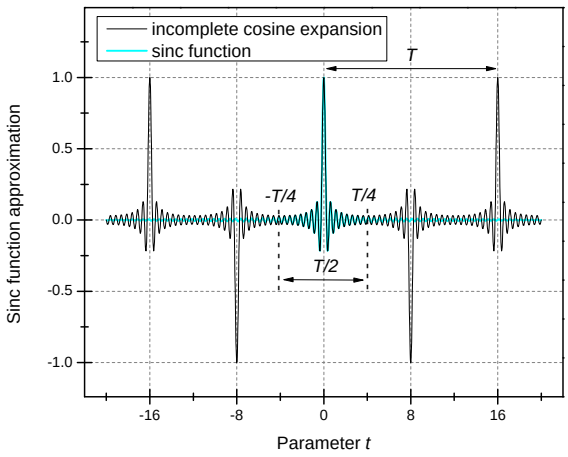

Fig. 1. The incomplete cosine expansion series at $M = 5$ and $h = 0.25$. The blue line shows the original sinc function $\operatorname{sinc}(\pi t/h)$.

It should be noted that approximation (6) is not the only incomplete cosine expansion of the sinc function. Examples of other incomplete cosine expansions are given in Appendix A.

2.2 The Voigt/complex error function

The efficiency of the incomplete cosine expansion can be demonstrated by application to the approximation of the complex error function defined as [27, 34]

$$w(z) = e^{-t^2}\left(1 + \frac{2i}{\sqrt{\pi}}\int_0^z e^{t^2}dt\right),$$

where $z = x + iy$ is a complex argument.

Numerical approximations of the complex error function, also known as the Faddeeva function, find broad applications in many fields of Physics, Astronomy and Chemistry and its efficient algorithmic implementation stills remains a hot topic (see, for example, optimized algorithm in a recent work [16]). Mathematically, the real part of the complex error function $K(x, y) = \mathrm{Re}[w(x, y)]$, widely known as the Voigt function [27, 34], represents a convolution of Cauchy (or Lorentz) and Gaussian (or Doppler) distributions. The Voigt function can be used to describe accurately spectral line broadening effects, for example, in atmospheric molecules [5, 24, 23], celestial bodies [8], photo-luminescent materials [20] and so on. The simultaneous Lorentz and Doppler broadenings occur primarily due to the Heisenberg uncertainty principle, multiple collisions between particles and the velocity distribution of colliding particles.

The imaginary part of the complex error function $L(x, y) = \mathrm{Im}[w(x, y)]$ is also a useful function that can be used, for example, to describe the spectral behavior of refractive index in dispersive materials [4, 7].

Plasma Physics involving small-amplitude waves propagating through Maxwellian media is based on the plasma dispersion function as given by [14, 30]

$$Z(z) \equiv \frac{1}{\sqrt{\pi}}\int_{-\infty}^{\infty}\frac{e^{-t^2}}{t - z}\,dt = i\sqrt{\pi}w(z).$$

The normal distribution function, applied in statistics and probability theory, can be expressed in terms of complex error function as [32]

$$\Phi(z) \equiv \frac{1}{\sqrt{2\pi}}\int_0^z e^{-x^2/2}dx = \frac{1}{2}\left[1 - e^{-z^2/2}w\left(\frac{iz}{\sqrt{2}}\right)\right].$$

The error function of complex argument can also be expressed in terms of complex error function as follows

$$\operatorname{erf}(z) = 1 - e^{-z^2} w(iz).$$

For example, the error function can be applied in a sub-pixel interpolation technique to star-image processing [25].

Consequently, the complex error function can be used as a versatile tool in Applied Mathematics and Computational Physics as the plasma dispersion function $Z(z)$, the normal distribution function $\Phi(z)$ and the error function $\operatorname{erf}(z)$ are simply the reformulated variations of the complex error function $w(z)$. Other functions that represent reformulations of the complex error function are the Fresnel integral [1, 19], the Dawson's integral [1, 19] and Gordeyev's integral [30, 18].

As we discussed above, the application of the sinc function may not be always efficient. One of the representations of the complex error function is given by (see equation (3) in [28], see also [2] for more details)

$$w(x,y) = \frac{1}{\sqrt{\pi}} \int_0^\infty \exp\left(-t^2/4\right) \exp(-yt) \exp(ixt)\, dt, \qquad y > 0. \tag{7}$$

Making change of variable $t/2 \to t$ in the integral (7) leads to [3]

$$w(x,y) = \frac{2}{\sqrt{\pi}} \int_0^\infty e^{-t^2} e^{2(ixt-yt)} dt, \qquad y > 0. \tag{8}$$

As we can see, the integrand in the integral (8) is a multivariable function. Obviously, this integrand can be rearranged as $f(t,x,y) = g(t)\, h(t,x,y) = e^{-t^2} e^{2(ixt-yt)}$, where $g(t) = e^{-t^2}$, $h(t,x,y) = e^{2(ixt-yt)}$. Consequently, according to equation (2) we can approximate equation (8) now as

$$w(x,y) \approx \frac{2}{\sqrt{\pi}} \sum_{n=-N}^{N} \int_0^\infty e^{-t_n^2} \operatorname{sinc}\left(\frac{\pi}{h}(t - t_n)\right) e^{2(ixt-yt)} dt, \qquad y > 0. \tag{9}$$

The most simplest way is to take equidistantly separated sampling points $t_n = nh$ with step between two adjacent sampling points equal to h. With

this assumption the approximation (9) yields

$$w\left(x,y\right)\approx\frac{2}{\sqrt{\pi}}\sum_{n=-N}^{N}\int_{0}^{\infty}e^{-n^{2}h^{2}}\mathrm{sinc}\left(\frac{\pi}{h}\left(t-nh\right)\right)e^{2(ixt-yt)}dt,\qquad y>0.\quad(10)$$

Although each integral term in the right side of equation (10) is integrable through hyperbolic arctangent function, this method is absolutely inappropriate for rapid computation since the resultant approximation of the complex error function is not a rational approximation.

This problem can be effectively resolved by using the incomplete cosine expansion. Specifically, we can write

$$e^{-t^{2}}\approx\frac{1}{2^{M-1}}\sum_{m=1}^{2^{M-1}}\sum_{n=-N}^{N}e^{-t_{n}^{2}}\cos\left(\frac{\pi\left(2m-1\right)\left(t-t_{n}\right)}{2^{M}h}\right),\qquad-T/4\leq t\leq T/4.\qquad(11)$$

Since the incomplete cosine expansion is a periodic function with period T, the obtained approximation (11) is also periodic as it can be seen in the Fig. 2. Along with the pick at the origin coinciding with original exponential function $e^{-t^{2}}$ shown by blue line, we can also observe additional negative and positive peaks at $t=\{\pm T/2,\pm3T/2,\pm5T/2\,,\pm7T/2\,...\}$ and $t=\{\pm T,\pm2T,\pm3T,\pm4T,\pm5T\,...\}$, respectively. Therefore, the exponential function $e^{-t^{2}}$ can be reasonably approximated only within the domain $-T/4\leq t\leq T/4$.

Let us introduce a real constant $\varsigma>0$ and multiply both sides of equation (11) by $e^{-\varsigma t}$. If the constant ς is large enough, say equal or greater than 2, the restriction $-T/4\leq t\leq T/4$ in equation (11) can be effectively eliminated as $e^{-\varsigma t}$ is a rapidly decreasing function that damps to zero all additional peaks as the argument t increases. This tendency can be observed from Fig. 3 by comparing two curves at $\varsigma=0.1$ and $\varsigma=0.2$ shown by black and red colors, respectively. As the constant ς increases, all additional peaks are attenuated significantly. By $\varsigma\gtrsim2$ they practically vanish and only the initial part of the approximated function $e^{-\varsigma t}e^{-t^{2}}$ remains unaffected. Thus, we can write

$$e^{-\varsigma t}e^{-t^{2}}\approx\frac{e^{-\varsigma t}}{2^{M-1}}\sum_{m=1}^{2^{M-1}}\sum_{n=-N}^{N}e^{-t_{n}^{2}}\cos\left(\frac{\pi\left(2m-1\right)\left(t-t_{n}\right)}{2^{M}h}\right),\qquad\varsigma\gtrsim2.\quad(12)$$

From equation (12) it follows that

$$e^{-\varsigma t}e^{-(t-\varsigma/2)^{2}}\approx\frac{e^{-\varsigma t}}{2^{M-1}}\sum_{m=1}^{2^{M-1}}\sum_{n=-N}^{N}e^{-t_{n}^{2}}\cos\left(\frac{\pi\left(2m-1\right)\left(t-t_{n}-\varsigma/2\right)}{2^{M}h}\right),\qquad\varsigma\gtrsim2.\qquad(13)$$

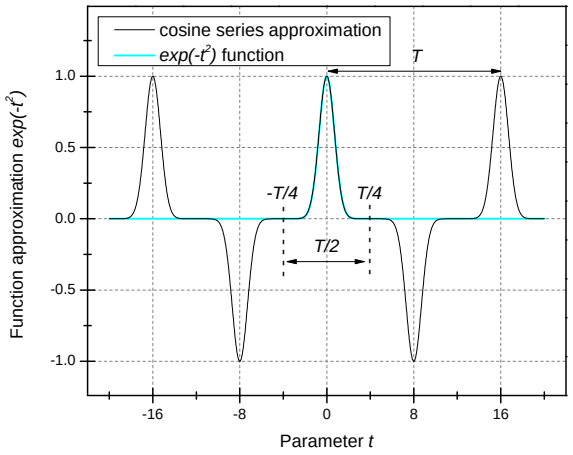

Fig. 2. Approximation of the function e^{-t^2} by incomplete cosine expansion at $M = 5$ and $h = 0.25$. The blue line shows the original function e^{-t^2}.

As the peak of the exponential function $e^{-(t-\varsigma/2)^2}$ is shifted to right from the origin by $\varsigma/2$, parameter ς can be regarded, therefore, as a shift constant.

Taking into account that $e^{-t^2} = e^{\varsigma^2/4} e^{-\varsigma t} e^{-(t-\varsigma/2)^2}$ and substituting approximation (13) into (8) leads to

$$w(x,y) \approx \frac{e^{\varsigma^2/4}}{2^{M-2}\sqrt{\pi}} \sum_{m=1}^{2^{M-1}} \sum_{n=-N}^{N} \int_0^{\infty} e^{-t_n^2} \cos\left(\frac{\pi(2m-1)(t-t_n-\varsigma/2)}{2^M h}\right) e^{-\varsigma t} e^{2(ixt-yt)} dt. \qquad (14)$$

Once again, assuming equidistant separation of the sampling points $t_n = nh$, we can rewrite approximation (14) in form

$$w(x,y) \approx \frac{e^{\varsigma^2/4}}{2^{M-2}\sqrt{\pi}} \sum_{m=1}^{2^{M-1}} \sum_{n=-N}^{N} \int_0^{\infty} e^{-n^2h^2} \cos\left(\frac{\pi(2m-1)(t-nh-\varsigma/2)}{2^M h}\right) e^{-\varsigma t} e^{2(ixt-yt)} dt. \qquad (15)$$

Each integral term on the right side of approximation (15) is now integrable and can be expressed as a rational function. Consequently, from equation (15) it follows that

$$w(z) \approx \sum_{m=1}^{2^{M-1}} \sum_{n=-N}^{N} \frac{\alpha_{m,n} + (z + i\varsigma/2)\beta_{m,n}}{C_m^2 - (z + i\varsigma/2)^2}, \qquad \mathrm{Im}[z] > 0, \qquad (16)$$

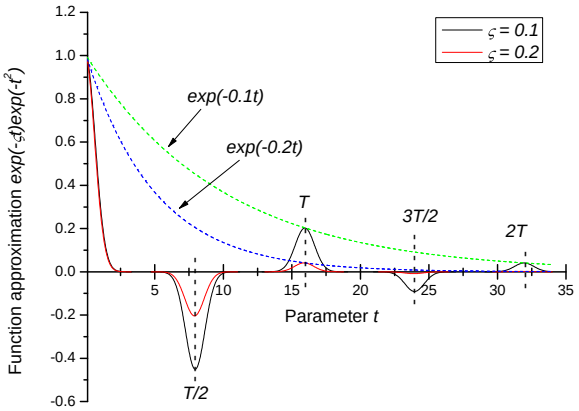

Fig. 3. Approximation of the function $e^{-\varsigma^2}e^{-t^2}$ by sampling with incomplete cosine expansion at $\varsigma = 0.1$ and $\varsigma = 0.2$ shown by black and red curves, respectively.

where

$$C_m = \frac{\pi\,(2m-1)}{2^{M+1}h},$$

$$\alpha_{m,n} = \frac{\sqrt{\pi}\,(2m-1)\,e^{\varsigma^2/4-n^2h^2}}{2^{2M}h}\sin\left(\frac{\pi\,(2m-1)\,(nh+\varsigma/2)}{2^{M}h}\right)$$

and

$$\beta_{m,n} = -i\frac{e^{\varsigma^2/4-n^2h^2}}{2^{M-1}\sqrt{\pi}}\cos\left(\frac{\pi\,(2m-1)\,(nh+\varsigma/2)}{2^{M}h}\right).$$

Although the approximation (16) is accurate, it is not rapid due to the double summation. However, this problem can be readily resolved by defining the following constants

$$A_m \equiv \sum_{n=-N}^{N}\alpha_{m,n}$$

and

$$B_m \equiv \sum_{n=-N}^{N}\beta_{m,n}.$$

Thus, after some trivial rearrangement we obtain

$$w(z) \approx \sum_{m=1}^{2^{M-1}} \frac{A_m + (z + i\varsigma/2) B_m}{C_m^2 - (z + i\varsigma/2)^2}, \qquad \mathrm{Im}[z] > 0, \tag{17}$$

where

$$A_m = \frac{\sqrt{\pi}(2m-1)}{2^{2M}h} \sum_{n=-N}^{N} e^{\varsigma^2/4 - n^2h^2} \sin\left(\frac{\pi(2m-1)(nh + \varsigma/2)}{2^M h}\right)$$

and

$$B_m = -\frac{i}{2^{M-1}\sqrt{\pi}} \sum_{n=-N}^{N} e^{\varsigma^2/4 - n^2h^2} \cos\left(\frac{\pi(2m-1)(nh + \varsigma/2)}{2^M h}\right).$$

Approximation (17) is a rational function since it contains no trigonometric or exponential functions dependent on the input parameters x and y. Furthermore, all coefficients A_m, B_m and C_m involved in computation are independent of the input parameters x and y. Therefore, the application of the approximation (17) is advantageous for rapid computation.

A further advantage is that the approximation (17) is readily integrable with respect to parameter x. As a result, it can be used for the spectrally integrated (or frequency integrated) Voigt function [6, 23].

It should be noted that for program coding the approximation (17) can be conveniently rearranged in form

$$w(z) \approx \psi(z + i\varsigma/2),$$

where

$$\psi(z) \equiv \sum_{m=1}^{2^{M-1}} \frac{A_m + zB_m}{C_m^2 - z^2}$$

is defined in order to deal with simplified $\psi(z)$-function.

To estimate the accuracy of this approximation (17), we define the relative errors for its real and imaginary parts as

$$\Delta_{\mathrm{Re}} = \left| \frac{\mathrm{Re}[w(x,y)] - \mathrm{Re}[w_{ref.}(x,y)]}{\mathrm{Re}[w_{ref.}(x,y)]} \right|$$

and

$$\Delta_{\mathrm{Im}} = \left| \frac{\mathrm{Im}\left[w\left(x,y\right)\right] - \mathrm{Im}\left[w_{ref.}\left(x,y\right)\right]}{\mathrm{Im}\left[w_{ref.}\left(x,y\right)\right]} \right|,$$

where $w_{ref.}\left(x,y\right)$ is the reference. The highly accurate reference values can be generated by using, for example, the program codes Algorithm 680 [21, 22] or recently published Algorithm 916 [34].

At sufficiently large value $|z|$, say at $|x+iy| \gtrsim 15$, the computation of the complex error function is not problematic and many approximations are available in scientific literature for rapid and accurate computation (see, for example, the continuous fractional approximation in [9], the Gauss–Hermit quadrature [11] or rational approximation in [12]). Since in quantitative spectroscopy the range for the input parameters required for computation is $0 < x < 40,000$ and $10^{-4} < y < 10^{2}$ [33, 24], the most difficult domain for computation is $0 < x < 15$ and $10^{-4} < y < 15$. The proposed approximation (17) of the complex error function very accurately covers this domain.

Figure 4a shows the logarithm of the relative error $\log_{10}\Delta_{\mathrm{Re}}$ for the real part of the complex error function approximation (17) calculated at $h = 0.25$, $N = 23$, $M = 5$ and $\varsigma = 2.75$. In the most of the domain, the accuracy in real part is better than 10^{-12}. Although in the real part the accuracy deteriorates at $y < 10^{-4}$, it still remains high and in the region $10^{-4} < y < 10^{-6}$ it is better than 10^{-8}.

Figure 4b illustrates the logarithm of the relative error $\log_{10}\Delta_{\mathrm{Im}}$ for the imaginary part of the complex error function approximation (17) also computed at $h = 0.25$, $N = 23$, $M = 5$ and $\varsigma = 2.75$. In the most of the domain, the accuracy in imaginary part is better than 10^{-12}. The accuracy deteriorates at $x < 10^{-4} \cup y < 10^{-4}$, but it is still high and better than 10^{-8}. It should be noted that in radiative transfer spectroscopy the accuracy better than 10^{-8} is more than enough for practical applications.

Consider the Weideman's approximation (see equation (38-I) and corresponding Matlab code in [31])

$$w\left(z\right) \approx \frac{\pi^{-1/2}}{L-iz} + \frac{2}{\left(L-iz\right)^{2}} \sum_{n=0}^{N-1} \gamma_{n+1} \left(\frac{L+iz}{L-iz}\right)^{n}, \qquad \mathrm{Im}\left[z\right] > 0, \qquad (18)$$

where $L = 2^{-1/4}N^{1/2}$ and

$$\gamma_{n} = \frac{L}{\pi} \int_{-\infty}^{\infty} e^{-t^{2}} \left(\frac{L-iz}{L+iz}\right)^{n} dt$$

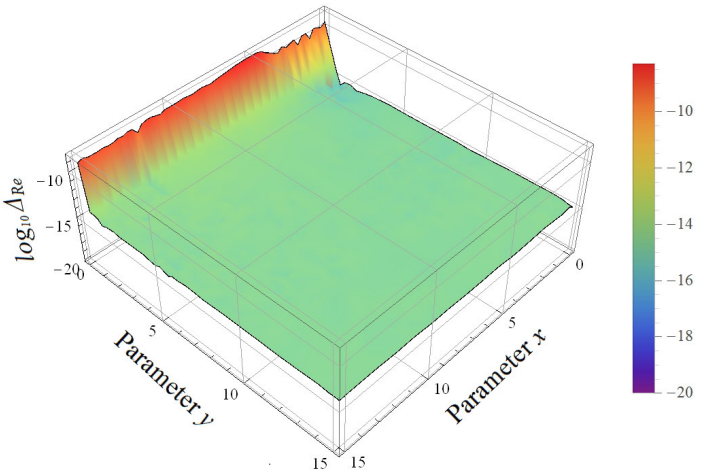

Fig. 4a. Logarithm of the relative error $\log_{10}\Delta_{\mathrm{Re}}$ for the real part of approximation (17) in the range $0 < x < 15$ and $10^{-6} < y < 15$.

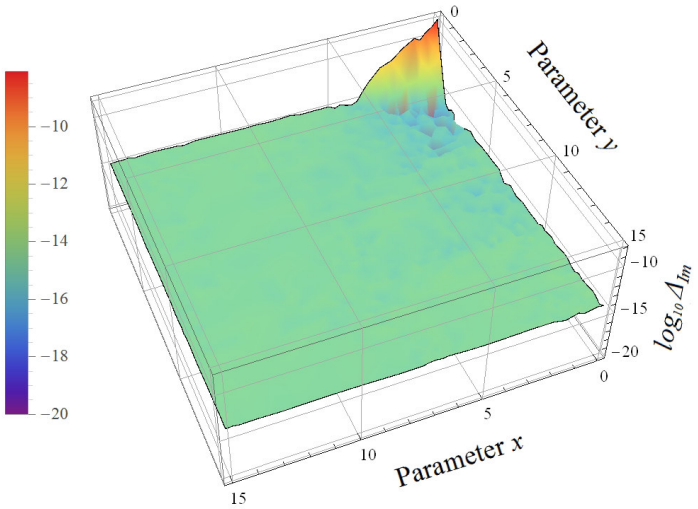

Fig. 4b. Logarithm of the relative error $\log_{10}\Delta_{\mathrm{Im}}$for the imaginary part of approximation (17) in the range $0 < x < 15$ and $10^{-6} < y < 15$.

are the expansion coefficients that can be determined elegantly by FFT method. As Weideman's approximation (18) is a rational function, it is rapid in computation and, therefore, widely used in many applications. By default, Weideman applied the integer $N = 16$ in equation (18).

Figure 5a shows the logarithm of the relative error $\log_{10}\Delta_{\mathrm{Re}}$ for the real part of the complex error function approximation (18). In the most of the domain in real part the accuracy is about 10^{-7} and deteriorates at $y < 10^{-4}$. Specifically, in the region $10^{-4} < y < 10^{-6}$ the accuracy cannot be better than 10^{-4}.

Figure 5b illustrates the logarithm of the relative error $\log_{10}\Delta_{\mathrm{Im}}$ for the imaginary part of the complex error function approximation (18). The accuracy in the imaginary part is essentially better. Particularly, the accuracy in the most of the domain is about 10^{-9} and deteriorates to 10^{-5} in the region $10^{-4} < y < 10^{-6}$.

As compared to the Weideman's approximation (18), the approximation (17) is more rapid in computation especially at extended size of the input array $\mathbf{z} = \{z_1, z_2, z_3 \ldots\}$. This is because the Weideman's approximation (18) is dependent on the power n. As a result of the exponentiations in polynomial terms, the Weideman's approximation (18) requires more computational resources when the size of the input array $\mathbf{z}$ exceeds several million elements.

Comparing Figs. 4a, 4b with 5a, 5b, one can see that while both approximations use 16 summation terms ($2^{5-1} = 16$ in approximation (17) and $N = 16$ in approximation (18)), the complex error function approximation (17) based on incomplete cosine expansion is more accurate than the Weideman's approximation by several orders of the magnitude. These results illustrate that the application of the incomplete cosine expansion to a challenging problem can produce a highly accurate and efficient functional approximation.

3 Conclusion

We present a method of functional approximation based on incomplete cosine expansion series as a practical alternative to the traditional sinc function sampling. Our analysis shows that applying this approach to the complex error function we obtain an approximation that with same numbers of summation terms provides better accuracy than Weideman's approximation by several orders of the magnitude. As application of the incomplete cosine ex-

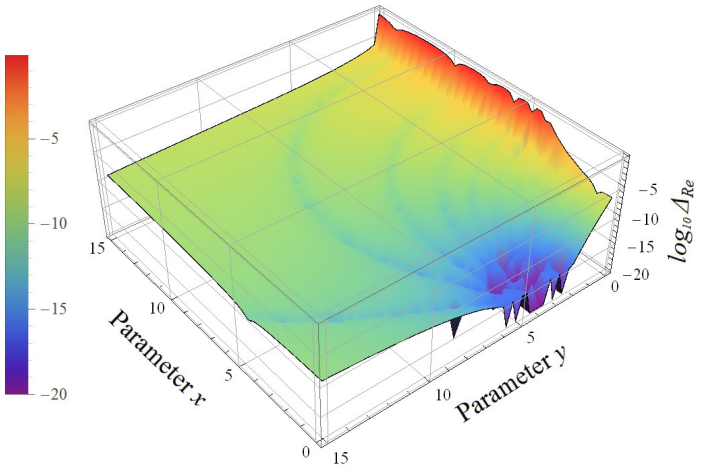

Fig. 5a. Logarithm of the relative error $\log_{10}\Delta_{\mathrm{Re}}$ for the real part of Weideman's approximation (18) in the range $0 < x < 15$ and $10^{-6} < y < 15$.

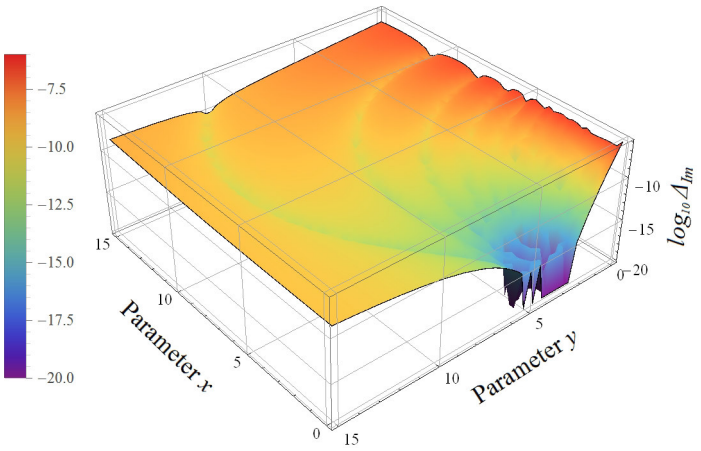

Fig. 5b. Logarithm of the relative error $\log_{10}\Delta_{\mathrm{Im}}$ for the imaginary part of Weideman's approximation (18) in the range $0 < x < 15$ and $10^{-6} < y < 15$.

pansion results in integration with only elementary functions, the approach is amenable to further mathematical flexibility and advantageous for accurate and rapid computation.

Acknowledgments

This work is supported by Thoth Technology Inc., Discovery Channel Canada and York University.

Appendix A

Since

$$\cos\left(\frac{2m-1}{2^M}t\right) = \cos\left(\frac{m-1/2}{2^{M-1}}t\right)$$

the sinc function can also be represented as the limit

$$\operatorname{sinc}(t) = \lim_{L\to\infty} \frac{1}{L}\sum_{\ell=1}^{L} \cos\left(\frac{\ell-1/2}{L}t\right).$$

This signifies that the upper value in summation may not be necessarily equal to 2^{M-1} and, in general, it can be taken as an arbitrary integer L:

$$\frac{1}{L}\sum_{\ell=1}^{L} \cos\left(\frac{\pi\,(\ell-1/2)}{Lh}t\right) \approx \operatorname{sinc}\left(\frac{\pi}{h}t\right), \qquad -T_L/4 \le t \le T_L/4, \tag{A.1}$$

where T_L is the corresponding period that increases with increasing integer L. The equation (6) is a specific case of a generalized equation (A.1) that occurs at $L = 2^{M-1}$.

Another expansion of the sinc function can be readily obtained by using the Poisson summation formula:

$$\sum_{p=-\infty}^{p=\infty} \operatorname{sinc}(t + pT_P) = \frac{\pi}{T_P} \sum_{p=-\lfloor T_P/(2\pi)\rfloor}^{\lfloor T_P/(2\pi)\rfloor} \cos\left(\frac{2\pi p}{T_P}t\right) \tag{A.2}$$

where notation $\lfloor\ \rfloor$ denotes the floor function and T_P is the corresponding period. From this equation we obtain the following incomplete cosine expan-

sion

$$\operatorname{sinc}(t) \approx \frac{\pi}{T_P} \sum_{p=-\lfloor T_P/(2\pi)\rfloor}^{\lfloor T_P/(2\pi)\rfloor} \cos\left(\frac{2\pi p}{T_P} t\right), \qquad -T_P/2 \leqslant t \leqslant T_P/2.$$

It is interesting to note that from equation (A.2) it follows that

$$\sum_{p=-\infty}^{\infty} \operatorname{sinc}(t + pT_P) = \frac{\pi}{T_P}, \qquad 0 < |T_P| < 2\pi$$

and at $T_P = 1$ we obtain an identity for the constant π:

$$\sum_{p=-\infty}^{\infty} \operatorname{sinc}(t + p) = \pi.$$

References

[1] M. Abramowitz and I.A. Stegun. Error Function and Fresnel Integrals. Handbook of mathematical functions with formulas, graphs, and mathematical tables. 9th ed. New York: Dover 1972.

[2] S.M. Abrarov and B.M. Quine, Efficient algorithmic implementation of the Voigt/complex error function based on exponential series approximation. Appl. Math. Comput. 218 (2011) 1894-1902. http://dx.doi.org/10.1016/j.amc.2011.06.072

[3] S.M. Abrarov and B.M. Quine, Master-slave algorithm for highly accurate and rapid computation of the Voigt/complex error function. J. Math. Research 6 (2014) 104-119. http://dx.doi.org/10.5539/jmr.v6n2p104

[4] N.L. Balazs and I. Tobias. Semiclassical dispersion theory of lasers. Phil. Trans. Royal Soc. A., 264 (1969) 129. http://dx.doi.org/10.1098/rsta.1969.0002

[5] A. Berk, Voigt equivalent widths and spectral-bin single-line transmittances: Exact expansions and the MODTRAN®5 implementation. J. Quant. Spectrosc. Radiat. Transfer, 118 (2013) 102-120. http://dx.doi.org/10.1016/j.jqsrt.2012.11.026

[6] D. Brüggemann, and M. Bollig, An efficient algorithm for frequency integration of Voigt profiles. J. Quant. Spectrosc. Radiat. Transfer, 48(1) (1992) 111-114. http://dx.doi.org/10.1016/0022-4073(92)90011-R

[7] L.K.P. Chan. Equation of atomic resonance for solid-state optics. Applied Optics, 25 (1986) 1728-730. http://dx.doi.org/10.1364/AO.25.001728

[8] D. Emerson, Interpreting Astronomical spectra. John Wiley & Sons Ltd. 1996.

[9] W. Gautschi, Efficient computation of the complex error function, SIAM J. Numer. Anal., 7 (1970) 187-198. http://www.jstor.org/stable/2949591

[10] W.B. Gearhart and H.S. Shultz, The function sin(x)/x, College Math. J, 21 (1990) 90-99. http://www.jstor.org/stable/2686748

[11] J. Humlíćek, An efficient method for evaluation of the complex probability function: the Voigt function and its derivatives. J. Quant. Spectrosc. Radiat. Transfer, 21 (1979) 309-313. http://dx.doi.org/10.1016/0022-4073(79)90062-1

[12] A.K. Hui, B.H. Armstrong and A.A. Wray, Rapid computation of the Voigt and complex error functions J. Quant. Spectrosc. Radiat. Transfer, 19 (1978) 509-516. http://dx.doi.org/10.1016/0022-4073(78)90019-5

[13] V.N. Faddeyeva and N.M. Terentev, Tables of the probability integral for complex argument, Pergamon Press, Oxford, 1961.

[14] B.D. Fried and S.D. Conte, The plasma dispersion function. New York: Academic Press 1961.

[15] M. Kac, Statistical independence in probability, analysis and number theory. Carus Monographs no. 12. Washington DC: Mathematical Association of America, 1959.

[16] T.M. Karbach, G. Raven and M. Schiller, Decay time integrals in neutral meson mixing and their efficient evaluation, http://arxiv.org/abs/1407.0748.

[17] F.G. Lether, Shifted rectangular quadrature rule approximations to Dawson's integral F(x), J. Comput. Appl. Math., 92 (1998) 97-102. http://dx.doi.org/10.1016/S0377-0427(98)00019-3

[18] R.L. Mace, A Gordeyev integral for electrostatic waves in a magnetized plasma with a kappa velocity distribution, Phys. Plasmas 10 (2003) 2181-2193. http://dx.doi.org/10.1063/1.1570828

[19] S.J. McKenna, A method of computing the complex probability function and other related functions over the whole complex plane, Astrophys. Space Sci., 107 (1984) 71-83. http://dx.doi.org/10.1007/BF00649615

[20] Y. Miyauchi, M. Iwamura, S. Mouri, T. Kawazoe, M. Ohtsu, and K. Matsuda, Brightening of excitons in carbon nanotubes on dimensionality modification. Nature Photonics, 7 (2013) 715-19. http://dx.doi.org/10.1038/nphoton.2013.179

[21] G.P.M. Poppe and C.M.J. Wijers, More efficient computation of the complex error function, ACM Transact. Math. Software, 16 (1990) 38-46. http://dx.doi.org/10.1145/77626.77629

[22] G.P.M. Poppe and C.M.J. Wijers, Algorithm 680: evaluation of the complex error function, ACM Transact. Math. Software, 16 (1990) 47. http://dx.doi.org/10.1145/77626.77630

[23] B.M. Quine and S.M. Abrarov, Application of the spectrally integrated Voigt function to line-by-line radiative transfer modelling, J. Quant. Spectrosc. Radiat. Transfer, 127 (2013) 37-48. http://dx.doi.org/10.1016/j.jqsrt.2013.04.020

[24] B.M. Quine and J.R. Drummond, GENSPECT: a line-by-line code with selectable interpolation error tolerance, J. Quant. Spectrosc. Radiat. Transfer, 74 (2002) 147-165. http://dx.doi.org/10.1016/S0022-4073(01)00193-5

[25] B.M. Quine, V. Tarasyuk, H. Mebrahtu and R. Hornsey, Determining star-image location: a new sub-pixel interpolation technique to process image centroids, Comp. Phys. Commun., 177 (2007) 700-706. http://dx.doi.org/10.1016/j.cpc.2007.06.007

[26] G.B. Rybicki, Dawson's integral and the sampling theorem, Comp. Physics 3 (1989) 85-87. http://dx.doi.org/10.1063/1.4822832

[27] F. Schreier, The Voigt and complex error function: A comparison of computational methods, J. Quant. Spectrosc. Radiat. Transfer, 48 (1992) 743-762. http://dx.doi.org/10.1016/0022-4073(92)90139-U

[28] H.M. Srivastava and M.P. Chen, Some unified presentations of the Voigt functions, Astrophys. Space Sci., 192 (1992) 63-74. http://dx.doi.org/10.1007/BF00653260

[29] F. Stenger, Handbook of sinc numerical methods, 2nd ed. Chapman & Hall/CRC 2011.

[30] D.G. Swanson, Plasma waves, 2nd ed. Auburn University, USA, IOP Publishing Ltd. 2003.

[31] J.A.C. Weideman, Computation of the complex error function. SIAM Journal on Numerical Analysis, 31 (1994) 1497-1518. http://www.jstor.org/stable/2158232

[32] E.W. Weisstein, CRC Concise Encyclopedia of Mathematics, 2nd ed., Chapman & Hall/CRC 2003.

[33] R.J. Wells, Rapid approximation to the Voigt/Faddeeva function and its derivatives. J. Quant. Spectrosc. Radiat. Transfer, 62 (1999) 29-48. http://dx.doi.org/10.1016/S0022-4073(97)00231-8

[34] M.R. Zaghloul and A.N. Ali, Algorithm 916: computing the Faddeyeva and Voigt functions, ACM Trans. Math. Software 38 (2011) 15:1-15:22. http://dx.doi.org/10.1145/2049673.2049679